Eur Biophys J (2014) 43:415–422
DOI 10.1007/s00249-014-0973-x

ORIGINAL PAPER

EBSA
Biophysics in Europe

F-subunit reinforces torque generation in V-ATPase

Jun-ichi Kishikawa · Akihiko Seino · Atsuko Nakanishi · Naciye Esma Tirtom · Hiroyuki Noji · Ken Yokoyama · Kumiko Hayashi

Received: 31 March 2014 / Revised: 15 May 2014 / Accepted: 29 May 2014 / Published online: 11 July 2014

Abstract Vacuolar-type H^+-pumping ATPases (V-ATPases) perform remarkably diverse functions in eukaryotic organisms. They are present in the membranes of many organelles and regulate the pH of several intracellular compartments. A family of V-ATPases is also present in the plasma membranes of some bacteria. Such V-ATPases function as ATP-synthases. Each V-ATPase is composed of a water-soluble domain (V_1) and a membrane-embedded domain (V_o). The ATP-driven rotary unit, V_1, is composed of A, B, D, and F subunits. The rotary shaft (the DF subcomplex) rotates in the central cavity of the A_3B_3-ring (the catalytic hexamer ring). The D-subunit, which has a coiled-coil domain, penetrates into the ring, while the F-subunit is a globular-shaped domain protruding from the ring. The minimal ATP-driven rotary unit of V_1 is comprised of the A_3B_3D subunits, and we therefore investigated how the absence of the globular-shaped F-subunit affects the rotary torque generation of V_1. Using a single-molecule technique, we observed the motion of the rotary motors. To obtain the torque values, we then analyzed the measured motion trajectories based on the fluctuation theorem, which states that the law of entropy production in non-equilibrium conditions and has been suggested as a novel and effective method for measuring torque. The measured torque of A_3B_3D was half that of the wild-type V_1, and full torque was recovered in the mutant V_1, in which the F-subunit was genetically fused with the D-subunit, indicating that the globular-shaped F-subunit reinforces torque generation in V_1.

Keywords V_1-ATPase · Torque generation · F-subunit · Fluctuation theorem

Introduction

Two types of rotary ATPases are present in various cellular membranes: V-ATPases and F-ATPases (Forgac 2007; Yokoyama and Imamura 2005; Yoshida et al. 2001). They couple both ATP synthesis and hydrolysis to proton translocation across the membrane by rotation of the rotary shaft in the catalytic hexamer ring (Fig. 1a). Overall, these ATPases possess a similar structure composed of a water-soluble domain (V_1 and F_1) and a membrane-embedded domain (V_o and F_0). Both domains can act as rotary motor proteins (Yoshida et al. 2001; Imamura et al. 2003).

The rotational catalysis of F_1 has been investigated in detail (Okuno et al. 2011). The minimal functional unit of F_1, which acts as the ATP-driven motor, is $\alpha_3\beta_3\gamma$ (Fig. 1a, left). The rotary shaft γ-subunit comprises a coiled-coil domain, and rotates in the central cavity of the $\alpha_3\beta_3$ ring by hydrolyzing ATP (Noji et al. 1997). Three β-subunits undergo ATP hydrolysis, and the conformation of the β-subunits changes as the elementary chemical

Electronic supplementary material The online version of this article (doi:10.1007/s00249-014-0973-x) contains supplementary material, which is available to authorized users.

J. Kishikawa · A. Nakanishi · K. Yokoyama
Kyoto Sangyo University, Kyoto 603-8555, Japan
e-mail: yokoken@cc.kyoto-su.ac.jp

A. Seino · K. Hayashi (✉)
Tohoku University, Sendai 980-8577, Japan
e-mail: kumiko@camp.apph.tohoku.ac.jp

N. E. Tirtom · H. Noji
University of Tokyo, Tokyo 113-8654, Japan

N. E. Tirtom
RIKEN, Yokohama 230-0045, Japan

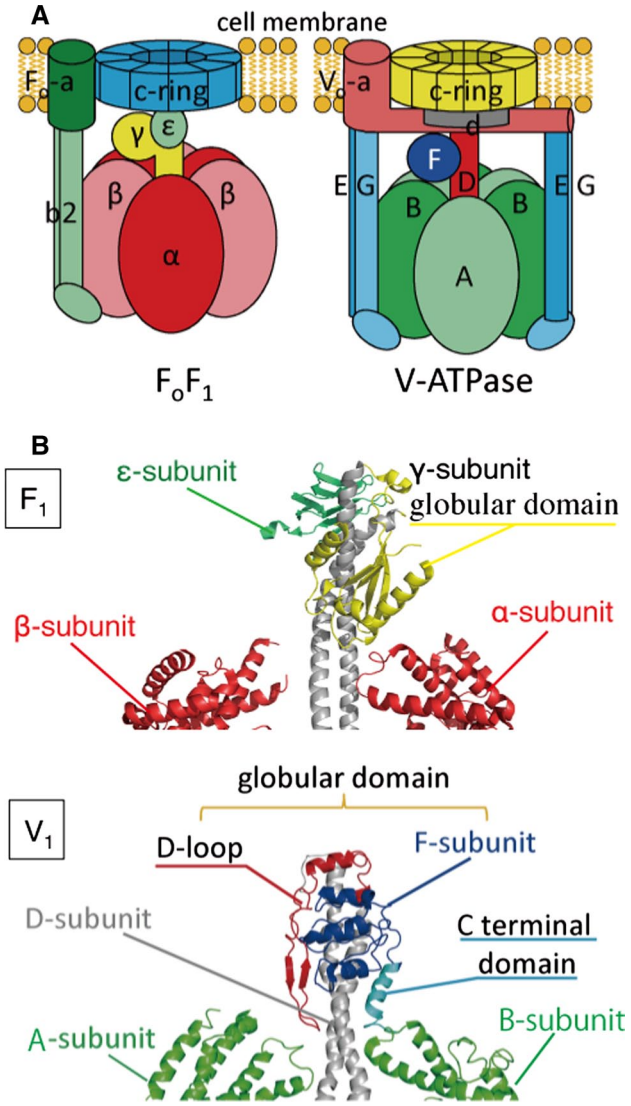

Fig. 1 **a** The schematics of F_0F_1 (*left*) and V_oV_1 (*right*). **b** The structures of the rotary shafts of F_1 (*top*, PDB:1H8E) and V_1 (*bottom*, PDB:3W3A). The α, β, ε and the globular domain of the γ-subunit are represented in *red, red, green*, and *yellow*, respectively in the case of F_1. The A, B, D, F, and D-loop, and the C-terminal domain of the F-subunit are represented in *green, green, gray, blue, red*, and *aqua*, respectively in the case of V_1. The globular domain of the rotary shaft consists of the F-subunit and the D-loop

steps involved in ATP hydrolysis proceed. The push-pull motion of the C-terminal domains of the β-subunit produces torque for the rotation of the γ-subunit (Wang et al. 1998). The torque generation efficiency of F_1, achieved by this push-pull motion, is nearly 100 %, far higher than other ATP-driven motors (Yasuda et al. 1998). The interaction between the globular domain of the γ-subunit and the C-terminal domain of the β-subunit plays a key role in reinforcing torque generation, and thus, in achieving this high efficiency (Usukura et al. 2012; Tanigawara et al. 2012). This interaction allows F_1 to generate torque and to rotate in the correct direction even when the coiled-coil domain of the shaft is truncated, leaving only the globular domain (Furuike et al. 2008).

However, compared to F_1, the rotary mechanisms of V_1, including the mechanism of torque generation, have not yet been fully elucidated, and V_1 has recently received increasing attention (Yokoyama and Imamura 2005; Kishikawa et al. 2013; Arai et al. 2013; Kishikawa et al. 2014; Nagamatsu et al. 2013). In V_1 (Fig. 1a, right), the rotary shaft (DF subcomplex), which contains a coiled-coil domain and a globular domain, as found in the γ-subunit of F_1, is thought to be a structural analog of the γ-subunit. The globular domain of the rotary shaft of V_1 is comprised of the F-subunit (Fig. 1b, blue) and the loop region of the D-subunit (Fig. 1b, red). In the present paper, we performed single-molecule experiments on V_1 to investigate how the absence of the globular domain of the rotary shaft in V_1 affects torque generation. First, we investigated a mutant in which the F-subunit had been deleted, A_3B_3D, which was reported to be the minimal rotary unit of V_1, as the ATP-driven motor (Imamura et al. 2004). Our single-molecule experiments showed that with a low ATP concentration, A_3B_3D rotated stepwise every 120° accompanied by a single ATP hydrolysis, and exhibited frequent 120° backward steps, which were seldom observed in the rotation of V_1. These backward steps were hypothesized to be caused by the absence of the F-subunit. To quantitate the effect of the absence of the F-subunit, we measured the torque of A_3B_3D by applying the fluctuation theorem (see Sect. 2.3), which is based on non-equilibrium statistical mechanics, and has recently been used to measure the torque of rotary motors (Usukura et al. 2012; Tanigawara et al. 2012; Hayashi et al. 2010, 2012; Hayashi and Hayashi 2012; Kim et al. 2011). We observed that A_3B_3D produced half the torque produced by V_1. This result indicates that the interaction between the hexamer ring and the globular domain of the shaft is important to generate full torque. Further, we created a mutant, $A_3B_3D_{\Delta loop}$, in which the loop region of the D-subunit (Fig. 1b, red) was deleted in addition to the F-subunit. The torque generated by $A_3B_3D_{\Delta loop}$ did not differ from that generated by A_3B_3D within the error margin of our experiments. Although the loop region of the D-subunit is also part of the globular domain of the rotary shaft, the region seems not to play an important role in torque generation, unlike the F-subunit. Finally, we constructed an expression vector for $A_3B_3DF_f$, containing a fusion of the genes coding for the D-subunit and the F-subunit, to mimic the γ-subunit of F_1. We observed that $A_3B_3DF_f$ generated as much torque as the wild-type V_1. This result is consistent with a previous report on the evolutionary relationship between the F-subunit of V_1 and the globular domain of the γ-subunit (Kishikawa et al. 2013).

Material and methods

Preparation of proteins

All mutant V_1 were constructed using a *T. thermophilus* His-tagged V_1 (A_3B_3DF) expression plasmid ($A_{(His-8/C28S/S232A/T235S/C255A/C508A)3}$ $B_{(C264S)3}$ $D_{(E48C/Q55C)}F$), as described in the Supplementary Material (Fig. S1). V_1 and the V_1 mutants were expressed in *Escherichia coli* cells. The *E. coli* cells were suspended in 100 mM sodium phosphate (pH 8.0), 200 mM NaCl, and 20 mM Imidazole, and disrupted by sonication, followed by heat treatment at 65 °C for 30 min. Following the removal of denatured *E. coli* proteins by centrifugation at 19,000×*g* for 60 min, the supernatant was subjected to Ni^{2+}-affinity chromatography (Qiagen) followed by ion exchange on a RESOURCE Q column (GE Healthcare). Purified samples were stored at 4 °C until use. The purified His-tagged enzymes were biotinylated at the two cysteines of the D-subunit with a five-fold molar excess of 6-{*N*′-[2-(*N*-maleimide)ethyl]-*N*-piperazinylamide}hexyl-D-biotinamide (Dojindo, Kumamoto, Japan) in 20 mM MOPS-KOH (pH 7.0) containing 100 mM KCl. After a 60-min incubation at 25 °C, the proteins were separated from the unbound reagent on a Superdex HR200 column equilibrated with 20 mM MOPS-NaOH (pH 7.0), containing 150 mM NaCl. The bound ADP in each enzyme was partially removed by successive EDTA-heat treatments.

Preparation of beads and rotation assay

The streptavidin-coated magnetic beads (100–300 nm) and the Ni^{2+}-NTA coated cover glass depicted in Fig. 2a were prepared as follows (Okuno et al. 2011). Because asymmetric-shaped beads are suitable for clear observation of the rotation of the motors, the magnetic beads were sonicated to produce asymmetric-shaped beads. Bead size had a broad distribution (100–300 nm).

Each flow cell (5–10 μl) was composed of two coverslips: a Ni^{2+}-NTA coated coverslip on the bottom (24 × 36 mm^2) and an untreated coverslip on the top (24 × 24 mm^2) separated by two spacers of 50-μm thickness (Fig. 2a). The biotinylated V_1 (or the V_1 mutants) (1–5 nM) in buffer A (50 mM Tris-Cl, pH 8.0, 100 mM KCl, and 2 mM $MgCl_2$) was applied to the flow cell and incubated for a few minutes at room temperature. Unbound enzymes were removed by washing with 20 μl of buffer A. Then, 20 μl of buffer A with 2 mg/ml BSA was infused into the flow cell and incubated for 30 s to prevent nonspecific binding. The BSA solution in the flow cell was removed by washing with 20 μl of buffer A. Then, buffer A containing the streptavidin-coated magnetic beads (10^7 particles/ml) was infused into the flow cell and incubated for a few minutes. Unbound beads were removed by washing with 20 μl of buffer A. Following the infusion of 80 μl of buffer A containing Mg-ATP at the indicated concentration (2 mM $MgCl_2$, 2.5 mM phosphoenol pyruvate, and 0.5 mg/ml pyruvate kinase), the rotation of a magnetic bead attached to a motor was recorded using a high-speed camera (Eclips, IN) at 1,000

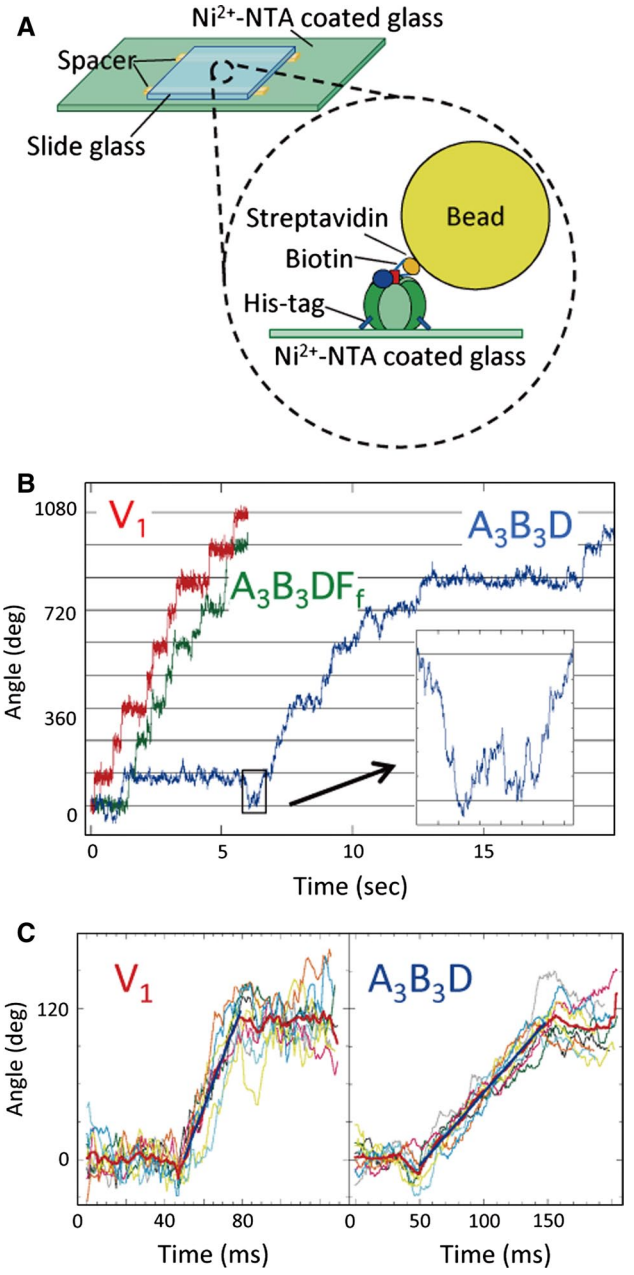

Fig. 2 **a** Schematic of the experimental setup (see Sect. 2.2 for details). **b** Rotary angle $\theta(t)$ plotted as a function of time for V_1 (*red*), A_3B_3D (*blue*), and $A_3B_3DF_f$ (*green*). The recording rate was 1,000 fps. **c** Ten trajectories of $\theta(t)$ during a 120° step were superposed to investigate angular velocities. The thick lines (*black*) show the averages over 10 trajectories. The slopes of the graphs correspond to the angular velocities

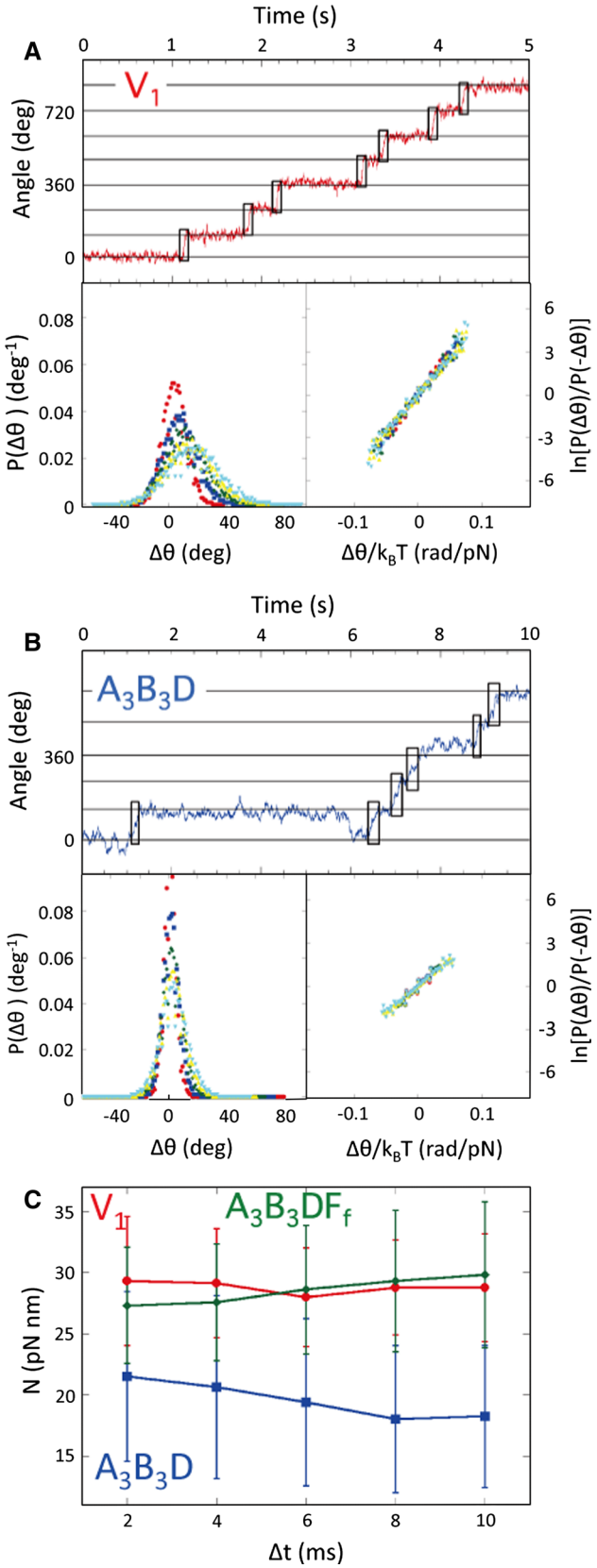

Fig. 3 The rotary angles $\theta(t)$ were plotted as a function of time for V_1 (**a**, *top*) and A_3B_3D (**b**, *top*) (the recording rate was 1,000 fps). From the probability distribution $P(\Delta\theta)$, where $\Delta\theta = \theta(t + \Delta t) - \theta(t)$ (**a**, **b**, *bottom, left*), the torque was calculated using the fluctuation theorem Eq. 2 that states $N = k_B T \ln[P(\Delta\theta)/P(-\Delta\theta)]/\Delta\theta$ (**a**, **b**, *bottom, right*) (See Supplementary Material for the detailed calculation). Each case is represented by a color: $\Delta t = 2$ ms (*red*), $\Delta t = 4$ ms (*blue*), $\Delta t = 6$ ms (*green*), $\Delta t = 8$ ms (*yellow*), and $\Delta t = 10$ ms (*aqua*). **c** Torque plotted as a function of Δt for V_1 (*red*), A_3B_3D (*blue*), and $A_3B_3DF_f$ (*green*). The *error bars* represent the standard deviations

frames per second (fps) using a phase-constant microscope (IX70, Olympus) with an −100 objective lens (N.A., 1.30, Olympus). Images were captured as a 32-bit AVI file. The centroid of the bead images was calculated.

Torque measurement method based on the fluctuation theorem

In our single-molecule experiments, the rotary torque was measured using the fluctuation theorem. The fluctuation theorem, which presents the statistical properties of entropy production in a small, non-equilibrium system, was first proposed in 1993 (Evans et al. 1993) [See Ref. (Ciliberto et al. 2010) for a review of the fluctuation theorem]. Recently, the fluctuation theorem has been suggested as a new method to measure the torque of rotary motor proteins (Usukura et al. 2012; Tanigawara et al. 2012; Hayashi et al. 2010, 2012; Hayashi and Hayashi 2012; Kim et al. 2011). In the present paper, we applied the theorem to measure the rotary torque of V_1 and its mutants.

In previous studies (Yasuda et al. 1998; Noji et al. 2001; Yasuda et al. 2001; Pänke et al. 2001), the rotary torque of a rotary motor, N, was estimated using the equation $N = \Gamma\omega$ where Γ and ω are the friction coefficient and mean angular velocity of a probe (e.g., a bead) attached to the rotary motor. Using fluid mechanics calculations, the functional forms of Γ were derived under the assumption that the rotation of the probe occurs in bulk. This results in inaccuracy when estimating Γ for single-molecule experiments using rotary motors. Because a rotary motor is attached to a glass slide and rotates the probe near the glass surface, the interaction between the probe and the glass causes the value of the friction coefficient estimated using fluid mechanics to differ from the actual value. In addition, in single-molecule experiments, probe sizes are sometimes distributed and their exact shapes are unknown (see Sect. 2.3 for the preparation of beads). To overcome this difficulty in estimating the friction coefficient of a probe, we use the fluctuation theorem, which aids in estimating N without using the value of Γ.

Table 1 The ratio of 120° backward steps to 120° forward steps

Sample	Backward/forward
V_1	6/776 (six molecules)
A_3B_3D	55/715 (seven molecules)
$A_3B_3DF_f$	6/697 (six molecules)

For a continuous rotation during a 120° forward step (as highlighted in black in Fig. 3a, b), assuming that the effect of inertia is small in the case of a probe attached to a rotary motor (see the experimental setup depicted in Fig. 2a), the time evolution of $\theta(t)$ is described by an over-damped Langevin equation

$$\Gamma\frac{d\theta}{dt} = N + \xi(t), \quad \left\langle \xi(t)\xi(t')\right\rangle = 2\Gamma k_B T\delta(t-t'), \qquad (1)$$

where ξ is a random force that represents the effect of thermal noise, k_B is the Boltzmann constant, and T is the room temperature. We also assumed that N is constant, as has been suggested in previous studies (Yasuda et al. 1998; Noji et al. 2001; Yasuda et al. 2001; Pänke et al. 2001). On the basis of the above model, the fluctuation theorem for torque measurement is expressed as

$$\ln[P(\Delta\theta)/P(-\Delta\theta)] = N\Delta\theta/k_B T, \qquad (2)$$

where $\Delta\theta = \theta(t+\Delta t) - \theta(t)$ and $P(\Delta\theta)$ are the probability distribution of $\Delta\theta$ (See Ref. (Hayashi et al. 2012) for the derivation of Eq. 2).

Results

Backward step and angular velocity

From the centroid of the bead attached to V_1, the rotary angle, θ, of the bead was calculated as a function of time. At a low ATP concentration (10 μM), V_1 rotated stepwise, pausing every 120° (Fig. 2b, red). Next, to elucidate the role of the globular domain of the rotary shaft, which is comprised of the F-subunit (Fig. 1b, blue) and the loop region of the D-subunit (Fig. 1b, red), the F-subunit deletion mutant, A_3B_3D, was investigated first. For A_3B_3D, we observed rotation (Fig. 2b, blue), but it often exhibited frequent 120° backward steps (Fig. 2b, inset), which were seldom observed in the rotation of the wild type V_1. The frequency of 120° backward steps for V_1 and A_3B_3D is summarized in Table 1. In Fig. 2c, the angular velocities of V_1 and A_3B_3D are shown; we observed that the angular velocity of A_3B_3D was significantly lower than that of V_1.

Rotary torque

To measure the rotary torque of V_1 and its mutants using the fluctuation theorem (Sect. 2.3), the probability distributions $P(\Delta\theta)$ were calculated for $\Delta t = 2.0$–10 ms, where $\Delta\theta = \theta(t+\Delta t) - \theta(t)$ (Fig. 3a, b, bottom, left. See the Supplementary Material for the calculation). Using these values, $P(\Delta\theta)$, $\ln[P(\Delta\theta)/P(-\Delta\theta)]$ was plotted as a function of $\Delta\theta/k_B T$ (Fig. 3a, b, bottom, right). The slopes of the graphs in Fig. 3a, b (bottom, right) correspond to the rotary torque values, N, according to Eq. 2. In Fig. 3c, it can be seen that N does not depend on Δt for 2 ms $\leq \Delta t$ within the error margins of our experiments. We regarded N in the case of $\Delta t = 10$ ms as the torque value of the motors (see Table S1 in the Supplementary Material for the torque values of all molecules). The torque value of the wild-type V_1 was 29 ± 4.4 (mean ± standard deviation) pNnm, which is consistent with previous studies (Hayashi et al. 2010; Imamura et al. 2005). For the F-subunit deletion mutant A_3B_3D, the torque value was estimated to be 18 ± 5.8 pNnm; this value was significantly lower than that of V_1. This indicates that the torque generation of V_1 was weakened by the absence of the F-subunit.

To elucidate which part of the F-subunit is most important for reinforcing torque generation, we further investigated the mutant ($A_3B_3DF_{\Delta Cterm}$) in which the C-terminal helix of the F subunit (Fig. 1b, aqua) was deleted. Note that a previous single-molecule study (Imamura et al. 2004) and a recent structure study (Arai et al. 2013) noted the importance of the interaction between the C-terminal helix of the F-subunit and the A_3B_3 ring for torque generation. For $A_3B_3DF_{\Delta Cterm}$, we obtained a low torque value (14 ± 2.8 pNnm), which is similar to that of the F-subunit deletion mutant A_3B_3D. The similarity of these values suggests that the lack of the interaction between the C-terminal helix of the F-subunit and the A_3B_3 ring most strongly influences torque generation.

Further, when the loop region of the D-subunit (Fig. 1b, red), which is also part of the globular domain of the rotary shaft, was deleted ($A_3B_3D_{\Delta loop}$) in addition to the F-subunit (i.e., the globular domain of the rotary shaft was fully removed in $A_3B_3D_{\Delta loop}$), we found that the torque value of $A_3B_3D_{\Delta loop}$ was 16 ± 3.7 pNnm. The fact that the torque value of $A_3B_3D_{\Delta loop}$ did not differ from that of A_3B_3D indicates that the absence of the loop region did not strongly affect torque generation, whereas the absence of the F-subunit did. The role of the loop region of the D-subunit may be to combine the D-subunit

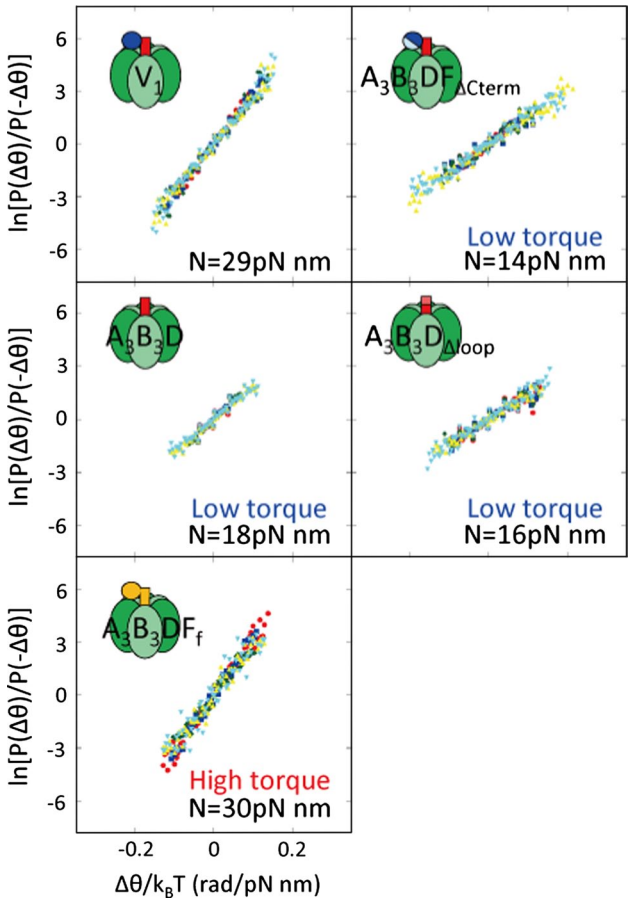

Fig. 4 Torque values obtained using Eq. 2 for V_1 (*top, left*), A_3B_3D (*middle, left*), $A_3B_3DF_f$ (*bottom, left*), $A_3B_3DF_{\Delta Cterm}$ (*top, right*), and $A_3B_3D_{\Delta loop}$ (*middle, right*). Each case is represented by a different color: $\Delta t = 2$ ms (*red*), $\Delta t = 4$ ms (*blue*), $\Delta t = 6$ ms (*green*), $\Delta t = 8$ ms (*yellow*), and $\Delta t = 10$ ms (*aqua*). See the Supplementary Material for the torque values of all molecules (Table S1)

with the F-subunit. The rotary torque measurements for V_1 and the V_1 mutants are summarized in Fig. 4.

Fused rotary shaft

The rotary shaft, γ-subunit of F_1, contains both helical and globular domains. In contrast, in V_1, these two domains are comprised of two separate subunits, the D-subunit and the F-subunit. Noting that our recent report suggested an evolutionary relationship between the F-subunit of V_1 and the globular domain of γ-subunit of F_1 (Kishikawa et al. 2013), we constructed an expression vector for $A_3B_3DF_f$ containing a fusion of the genes coding for the subunits D and F to mimic γ-subunit of F_1, which is a more advanced shaft. In this V_1 mutant, the F-subunit appeared artificially in the middle of the D-subunit (DF_f complex). Using a bulk assay, we observed that the ATPase activity of $A_3B_3DF_f$ was almost identical to that of the wild-type V_1 (Kishikawa et al. 2013). We also measured the torque of $A_3B_3DF_f$, which was not measured in the previous study (Kishikawa et al. 2013). We found that $A_3B_3DF_f$ exhibited high torque (30 ± 6.0 pNnm), as was observed in V_1 (Fig. 4, bottom). In addition, we seldom observed 120° backward steps in $A_3B_3DF_f$ (Table 1). These results, combined with the previously reported results (Kishikawa et al. 2013), indicate that the DF_f subunits function as a complete rotary shaft with respect to ATP-hydrolysis-driven torque generation.

Conclusion

In this study, we quantitatively investigated the importance of the globular domain of a rotary shaft from the viewpoint of ATP-hydrolysis-driven torque generation. Although a study of the crystal structure of V_1 (Arai et al. 2013) reported the possibility that the globular domain of the rotary shaft interacts with the A_3B_3 ring, the prediction was not quantitative. Our torque measurements made it clear that the effect of deleting the globular domain of the rotary shaft decreased torque by half. This degree of change is similar to that observed in F_1, in which the absence of the interaction between the rotary shaft and the ring also weakened torque generation (Usukura et al. 2012; Tanigawara et al. 2012).

In wild-type V_1, the globular domain of the rotary shaft is comprised of the F-subunit (Fig. 1b, blue) and the loop region of the D-subunit (Fig. 1b, red). First, we investigated an F-subunit deletion mutant, A_3B_3D. A_3B_3D often exhibited 120° backward steps (Fig. 2b; Table 1) and exerted half the torque of the wild-type V_1 (Fig. 3). The torque values observed for $A_3B_3DF_{\Delta Cterm}$, in which the C-terminal helix of the F-subunit was deleted, were similar to the value observed for A_3B_3D (Fig. 4). Based on these results, the F-subunit, particularly its C-terminal domain, plays an important role in the exertion of full torque. However, the loop region of the D-subunit, which is also part of the globular domain of the rotary shaft (Fig. 1b, red), is not significant for torque generation; the torque generated by $A_3B_3D_{\Delta loop}$, in which the loop region was also deleted from A_3B_3D, was identical to that generated by A_3B_3D (Fig. 4, middle, right).

In $A_3B_3DF_f$, in which the F-subunit was genetically fused with the D-subunit to mimic the γ-subunit of F_1, the rotary shaft DF_f was found to retain full function as a rotary shaft, in terms of torque generation (Fig. 4, bottom, left; Table 1). However, the V_o and $A_3B_3DF_f$ complex is known to be unable to synthesize ATP (data not shown), which indicates that in this complex, the torque is not fully transmitted from V_o to $A_3B_3DF_f$. Because the main part of the globular domain of the F-subunit appeared artificially in the middle of the D-subunit in the rotary shaft DF_f, the

function of this globular domain may differ from the original, particularly with respect to torque transmission. This indicates that the original globular domain of the rotary shaft is important to reinforce torque transmission, as well as torque generation. The role of the globular domain should be quantitatively investigated in future, from the viewpoint of torque transmission between V_o and V_1.

In the present study, we computed the rotary torque of V_1 using the fluctuation theorem. This method for torque measurement, based on non-equilibrium statistical mechanics, has been actively applied to single-molecule experiments on rotary motors (Usukura et al. 2012; Tanigawara et al. 2012; Hayashi et al. 2010, 2012; Hayashi and Hayashi 2012; Kim et al. 2011). The theorem enabled us to measure the rotary torque of V_1 without determining the value of the friction coefficient of the rotary probe (Sect. 2.3). Although our rotary probes (sonicated beads) were useful to visualize the rotary motion of the motors, because they were irregularly shaped, their friction coefficients could not be theoretically calculated using fluid mechanics (Hayashi et al. 2010). Because it is difficult to precisely measure friction coefficients in both in-vitro (Harada et al. 2001) and in-vivo (Hayashi et al. 2013) single-molecule experiments, it is important to broaden the applicability of the theorem to a wide range of biological motors to measure their force and torque. We hope that application of new relations of non-equilibrium statistical mechanics on non-equilibrium fluctuation (Hayashi et al. 2013; Mizuno et al. 2007; Toyabe et al. 2010; Liphardt et al. 2002; Collin et al. 2005; Alemany et al. 2012) will facilitate a better understanding of the mechanisms of biological motors, and that the present study contributes to this effort.

Acknowledgments This work was supported by Grants-in-Aid for Scientific Research to K. Y. and K. H. from the MEXT (Nos. 24370059 and 24770143). We thank T. Sagawa for providing the expertise required to use the torque measurement software, and the members of the Sasaki laboratory for their helpful discussions.

References

Alemany A, Mossa A, Junier I, Ritort F (2012) Experimental free-energy measurements of kinetic molecular states using fluctuation theorems. Nat Phys 8:688–694

Arai S, Saijo S, Suzuki K, Mizutani K, Kakinuma Y, Ishizuka-Katsura Y, Ohsawa N, Terada T, Shirouzu M, Yokoyama S, Iwata S, Yamato I, Murata T (2013) Rotation mechanism of *Enterococcus hirae* V_1-ATPase based on asymmetric crystal structures. Nature 493:703–707

Ciliberto S, Jouboud S, Petrosyan A (2010) Fluctuation in out-of-equilibrium systems: from theory to experiment. J Stat Mech P12003.

Collin D, Ritort F, Jarzynski C, Smith SB, Tinoco I Jr, Bustamante C (2005) Verification of the Crooks fluctuation theorem and recovery of RNA folding free energies. Nature 437:231–234

Evans DJ, Cohen EGD, Morriss GP (1993) Probability of second law violations in shearing steady states. Phys Rev Lett 71:2401–2404

Forgac M (2007) Vacuolar ATPases: rotary proton pumps in physiology and pathophysiology. Nat Rev Mol Cell Biol 8:917–929

Furuike S, Hossain MD, Maki Y, Adachi K, Suzuki T, Kohori A, Itoh H, Toshida M, Kinosita K Jr (2008) Axle-less F_1-ATPase rotates in the correct direction. Science 319:955–958

Harada Y, Ohara O, Takatsuki A, Itoh H, Shimamoto N, Kinosita K Jr (2001) Direct observation of DNA rotation during transcription by Escherichia coli RNA polymerase. Nature 409:113–115

Hayashi K, Ueno H, Iino R, Noji H (2010) Fluctuation theorem applied to F_1-ATPase. Phys Rev Lett 104:218103

Hayashi K, Tanigawara M, Kishikawa J (2012) Measurements of the driving forces of bio-motors using the fluctuation theorem. Biophysics 8:67–72

Hayashi K, Hayashi R (2012) Protein motor F as a model system for fluctuation theories of non-equilibrium statistical mechanics. Fluct Noise Lett 11:1241001

Hayashi K, Pack CG, Sato MK, Mouri K, Kaizu K, Takahashi K, Okada Y (2013) Viscosity and drag force involved in organelle transport: investigation of the fluctuation dissipation theorem. Eur Phys J E 36:136

Imamura H, Nakano M, Noji H, Muneyuki E, Okumura S, Yoshida M, Yokoyama K (2003) Evidence for rotation of V_1-ATPase. Proc Natl Acad Sci 100:2312–2315

Imamura H, Ikeda C, Yoshida M, Yokoyama K (2004) The F subunit of Thermus thermophilus V_1-ATPase promotes ATPase activity but is not necessary for rotation. J Biol Chem 279:18085–18090

Imamura H, Takeda M, Funamoto S, Shimabukuro K, Yoshida M, Yokoyama K (2005) Rotation scheme of V_1-motor is different from that of F_1-motor. Proc Natl Acad Sci 102:17929–17933

Kim Y, Konno H, Sugano Y, Hisabori T (2011) Redox regulation of rotation of the cyanobactrial F_1-ATPase containing thiol regulation switch. J Chem Biol 286:9071–9078

Kishikawa J, Ibuki T, Nakamura S, Nakanishi A, Minamino T, Miyata T, Namba K, Koono H, Ueno H, Imada K, Yokoyama K (2013) Common evolutionary origin for the rotor domain of rotary ATPases and flagellar protein export apparatus. PLos One 8:e64695

Kishikawa J, Nakanishi A, Furuike S, Tamakoshi M, Yokoyama K (2014) Molecular basis of ADP inhibition of vacuolar (V)-type ATPase/synthase. J Biol Chem 289:4003–4012

Liphardt J, Dumont S, Smith SB, Tinoco I Jr, Bustamante C (2002) Equilibrium information from nonequilibrium measurements in an experimental test of Jarzynski equality. Science 296:1832–1835

Mizuno D, Tardin C, Schmidt CF, MacKintosh FC (2007) Nonequilibrium mechanics of active cytoskeltal networks. Science 315:370–373

Nagamatsu Y, Takeda K, Kuranaga T, Numoto N, Miki K (2013) Origin of asymmetry at the intersubunit interfaces of V_1-ATPase from thermus thermophilus. J Mol Biol 425:2699–2708

Noji H, Yasuda R, Yoshida M, Kinosita K Jr (1997) Direct observation of the rotation of F_1-ATPase. Nature 386:299–302

Noji H, Blad D, Yasuda R, Itoh H, Yoshida M, Kinosita K Jr (2001) Purine but not pyrimidine nucleotides support rotation of F_1-ATPase. J Biol Chem 276:25480–25486

Okuno D, Lino R, Noji H (2011) Rotation and structure of F_0F_1-ATP synthase. J Biochem 149:655–664

Pänke O, Cherepanov DA, Gumbiowski K, Engelbrecht S, Junge W (2001) Viscoelastic dynamics of actin filaments coupled to rotary F-ATPase: angular torque profile of the enzyme. Biophys J 81:1220–1233

Tanigawara M, Tabata KV, Ito Y, Ito J, Watanabe R, Ueno H, Ikeguchi M, Noji H (2012) Role of the DELSEED loop in torque transmission of F_1-ATPase. Biophys J 103:970–978

Toyabe S, Okamoto T, Watanabe-Nakayama T, Taketani H, Kudo S, Muneyuki E (2010) Nonequilibrium energetics of a single F_1-ATPase molecule. Phys Rev Lett 104:198103

Usukura E, Suzuki T, Furuike S, Soga N, Saita E, Hisabori T, Kinosita K Jr, Yoshida M (2012) Torque generation and utilization in motor enzyme F_oF_1-ATP synthase. J Biol Chem 287:1884–1891

Wang H, Oster G (1998) Energy transduction in the F_1 motor of ATP synthase. Nature 396:279–282

Yasuda R, Noji H, Kinosita K Jr, Yoshida M (1998) F_1-ATPase is a highly efficient molecular motor that rotates with discrete 120° steps. Cell 93:1117–1124

Yasuda R, Noji H, Yoshida M, Kinosita K Jr, Itoh H (2001) Resolution of distinct rotational substeps by submillisecond kinetic analysis of F_1-ATPase. Nature 410:898–904

Yokoyama K, Imamura H (2005) Rotation, structure, and classification of prokaryotic V-ATPase. J Bioenerg Biomembr 37:405–410

Yoshida M, Muneyuki E, Hisabori T (2001) ATP synthase—a marvellous rotary engine of the cell. Nat Rev Mol Biol 2:669–677